

Dental Pulp-Derived CD31⁻/CD146⁻ Side Population Stem/Progenitor Cells Enhance Recovery of Focal Cerebral Ischemia in Rats

Masahiko Sugiyama, D.D.S.,^{1,2} Koichiro Iohara, Ph.D.,¹ Hideaki Wakita, Ph.D.,³ Hisashi Hattori, Ph.D.,² Minoru Ueda, Ph.D.,² Kenji Matsushita, Ph.D.,¹ and Misako Nakashima, Ph.D.¹

Regenerative therapy using stem cells is a promising approach for the treatment of stroke. Recently, we reported that CD31⁻/CD146⁻ side population (SP) cells from porcine dental pulp exhibit highly vasculogenic potential in hindlimb ischemia. In this study, we investigated the influence of CD31⁻/CD146⁻ SP cells after transient middle cerebral artery occlusion (TMCAO). Adult male Sprague-Dawley rats were subjected to 2 h of TMCAO. Twenty-four hours after TMCAO, CD31⁻/CD146⁻ SP cells were transplanted into the brain. Motor function and infarct volume were evaluated. Neurogenesis and vasculogenesis were determined with immunochemical markers, and the levels of neurotrophic factors were assayed with real-time reverse transcription–polymerase chain reaction. In the cell transplantation group, the number of doublecortin-positive cells increased twofold, and the number of NeuN-positive cells increased eightfold, as compared with the control phosphate-buffered saline group. The vascular endothelial growth factor level in the ischemic brain with transplanted cells was 28 times higher than that in the normal brain. In conclusion, CD31⁻/CD146⁻ SP cells promoted migration and differentiation of the endogenous neuronal progenitor cells and induced vasculogenesis, and ameliorated ischemic brain injury after TMCAO.

Introduction

SEVERAL PRECLINICAL STUDIES have provided evidence that transplanted stem cells have therapeutic potential in the treatment of stroke.¹ Stem cells have the capability to migrate to areas of injury and secrete neuroprotective factors to induce neurogenesis.² In the adult mammalian brain, neurogenesis persists in certain distinct regions of the central nervous system such as the subventricular zone (SVZ) and the dentate gyrus of the hippocampus.³ It has been reported that transplanting differentiated neural stem cells isolated from dental pulp improved motor disability and reduced infarct volume.⁴ However, the influence of transplanting stem/progenitor cells isolated from dental pulp in cerebral ischemia has not been elucidated. Recently, we reported that CD31⁻/CD146⁻ side population (SP) cells containing stem/progenitor cells from porcine dental pulp exhibit highly vasculogenic potential *in vitro* and promote revascularization in hindlimb ischemia.⁵ In the present study, we investigated the effects of these cells on neurogenesis and vasculogenesis in a cerebral ischemia model in a rat. In addition, the effects on the motor dysfunction and infarct volume were evaluated after transient middle cerebral artery occlusion (TMCAO).

Materials and Methods

Isolation of CD31⁻/CD146⁻ SP cells

CD31⁻/CD146⁻ SP and CD31⁺/CD146⁻ SP cells were isolated from porcine tooth germ, as described previously.⁵ CD31⁻/CD146⁻ SP cells were cultured in endothelial basal medium-2 (EBM-2, single quote cc-4176) with 10 ng/mL insulin-like growth factor 1 (IGF1), 10 ng/mL epidermal growth factor (EGF), and 10% fetal bovine serum (FBS). CD31⁺/CD146⁻ SP cells were cultured in EBM-2 with 10 ng/mL bFGF, 10 ng/mL vascular endothelial growth factor (VEGF), 138 nM hydrocortisone, 0.09 mg/mL heparin, 50 µg/mL ascorbic acid, and 10% FBS. They were routinely subcultured up to 70% confluence under identical conditions.

Cerebral ischemia model

All animal experiments were approved by the Institutional Animal Care and Use Committee (National Center for the Geriatrics and Gerontology). Adult male Sprague-Dawley rats (Japan SLC, Inc.) weighing 300–400 g were used. Animals were initially anesthetized with 5% isoflurane (Abbott Laboratories) and maintained under anesthesia with 1.5% isoflurane in a mixture of 70% N₂O and 30% O₂. Rectal

¹Department of Oral Disease Research, National Center for Geriatrics and Gerontology, Research Institute, Obu, Aichi, Japan.

²Department of Oral and Maxillofacial Surgery, Laboratory Medicine, Nagoya University Graduate School of Medicine, Nagoya, Japan.

³Department of Vascular Dementia Research, National Center for Geriatrics and Gerontology, Research Institute, Obu, Aichi, Japan.

temperature was maintained at $37^{\circ}\text{C} \pm 0.5^{\circ}\text{C}$ on a heating pad. Focal cerebral ischemia was induced by TMCAO with 2 h.⁶ A 4-0 monofilament nylon suture (Shirakawa) with the tip rounded by flame heating and silicone (KE-200; Shin-Etsu Chemical) was advanced from the external carotid artery into the internal carotid artery until it blocked the origin of the MCA. Two hours after occlusion, reperfusion was performed by withdrawal of the suture. The regional cerebral blood flow of the MCA territory was measured using a laser-Doppler flowmeter (Omega FLO-N1; Omega Wave, Inc.) after occlusion. The response was considered positive and included only if the reduction in regional cerebral blood flow was $>70\%$.

Transplantation

Twenty-four hours after TMCAO (day 0), the rats were again anesthetized with sodium pentobarbital (Schering-Plough) (0.25 mL/kg, intraperitoneally) and maintained under anesthesia with 1.5% isoflurane in a mixture of 70% N_2O and 30% O_2 . Animals were randomly divided into three groups: (I) $\text{CD31}^-/\text{CD146}^-$ SP cell transplantation group ($n=24$, day 3 sacrificed=6, day 9 sacrificed=7, day 21 sacrificed=11), (II) unfractionated pulp cell transplantation group ($n=4$, used for motor function), and (III) vehicle alone (phosphate-buffered saline [PBS]) group ($n=20$, day 3 sacrificed=6, day 9 sacrificed=5, day 21 sacrificed=9). The infarction site was targeted for transplantation at the striatum of the following coordinates: 1.0 mm rostral to the bregma, 6.0 mm lateral to the midline, 5.0 mm ventral to the dura (Fig. 1A, B). Subsequently, 1×10^6 $\text{CD31}^-/\text{CD146}^-$ SP cells or unfractionated pulp cells at the fifth to seventh passage after labeling with 1,1-dioctadecyl-3,3,3,3 tetramethylindocarbocyanine perchlorate (DiI; Sigma), and removing all added factors into each medium were diluted with 2 μL of PBS, and were transplanted by Hamilton microsyringe (Hamilton). The control group consisted of an equal volume of PBS injected into the same site.

Immunohistochemistry

At day 3 or 21 after injection, the rat was transcardially perfused with 4% paraformaldehyde solution (Nakarai Tesque). The brain was removed and postfixed in paraformaldehyde. The following day, it was immersed in 30% sucrose solution. Twelve-micrometer-thick coronal sections were cut on a cryostat. For immunohistochemistry, the sections were preincubated in blocking solution (PBS containing 5% normal serum of the species in which the secondary antibody was raised) for 2 h at room temperature, and incubated with primary antibodies diluted for 1 h at room temperature. The primary antibodies were as follows: neuronal progenitor cells (NPC) marker, rabbit anti-doublecortin (1:50; Abcam, Inc.); neuron marker, rabbit anti-neurofilament H (1:200; Chemicon) and mouse anti-NeuN (anti-neuronal nuclei, 1:500; Chemicon); endothelial cell marker, mouse anti-RECA1 (rat endothelial cell antigen; Monosan); apoptosis marker, rabbit anti-cleaved caspase-3 (1:50; Cell Signaling Technology, Inc.); and VEGF marker, rabbit anti-VEGF (VEGF [P-20]: sc-1836; Santa Cruz Biotech). After washing, sections were incubated for 1 h at room temperature with secondary antibodies (on day 21, for neurofilament H/doublecortin, Donkey anti-rabbit IgG FITC [1:400; Jackson ImmunoResearch]; for NeuN/RECA1, Goat anti-mouse IgG FITC [1:200; MP Biomedicals]; and for VEGF, rabbit anti-goat

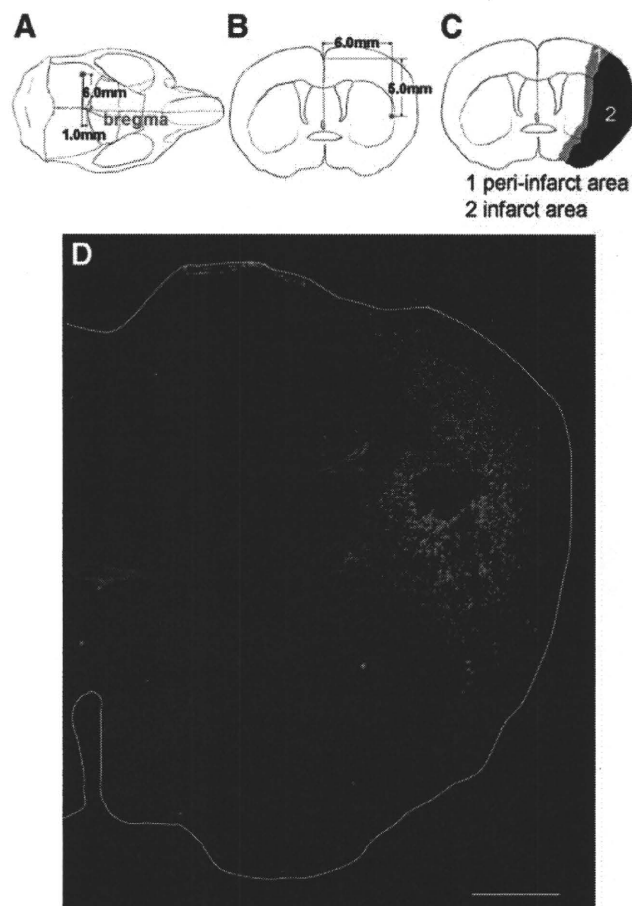


FIG. 1. (A) Overhead and (B) coronal view of the injection site. (C) The peri-infarct area. Peri-infarct area (gray), infarct core (black). (D) DiI-labeled transplanted $\text{CD31}^-/\text{CD146}^-$ SP cells (red) migrated from the original injection site to the peri-infarct area in the cortex and striatum. White outline is the outer circumference of brain. Scale bar = 1000 μm . SP, side population. DiI, 1,1-dioctadecyl-3,3,3,3 tetramethylindocarbocyanine perchlorate. Color images available online at www.liebertonline.com/tea

IgG-HRP [1:400; Invitrogen Corporation]. On day 3, for cleaved caspase-3, goat anti-rabbit IgG-HRP [1:400; Invitrogen] and for VEGF, rabbit anti-goat IgG-HRP [1:400; Invitrogen]. The sections with HRP-conjugated secondary antibodies were incubated in anti-fluorescein-HRP (1:400; TSATM Fluorescence Systems; PerkinElmer) for 7 min at room temperature. Adjacent sections were used as negative controls. In the control sections, all procedures were processed in the same manner except that the primary antibodies were omitted. To identify migration of NPC from SVZ, we observed the cryosections on days 9 and 21 with anti-doublecortin on fluorescence microscope (BZ-9000; Keyence) and BZ-HIC (Keyence).

Statistical analyses of the density of cells

The density of NPCs, neurons, endothelial cells, and apoptotic cells in the peri-infarct area (Fig. 1C) and the contralateral region in the $\text{CD31}^-/\text{CD146}^-$ SP cell transplantation group and PBS groups were determined. In all groups (PBS group, $\text{CD31}^-/\text{CD146}^-$ SP cell transplantation group,

TABLE 1. PORCINE PRIMERS FOR REAL-TIME REVERSE TRANSCRIPTION-POLYMERASE CHAIN REACTION AND *IN SITU* HYBRIDIZATION

Gene		5' DNA sequence 3'	Product size (bp)	Accession no.
r.β-actin	Forward	AAGTACCCCATGAACACGG	257	NM_031144
	Reverse	ATCACAATGCCAGTGGTACG		
p.β-actin	Forward	CTGGGGCCTAACGTTCTCAC	198	BI118314
	Reverse	GTCCTTTCTTCCCGATGTT		
VEGF	Forward	ATGGCAGAAGGAGACCAGAA	224	MN_214084
	Reverse	ATGGCGATGTTGAACTCCTA		
BDNF	Forward	TTCAAGAGGCCTGACATCGT	180	MN_214259
	Reverse	AGAAGAGGAGGCTCCAAAGG		
NGF	Forward	TGGTGTGGGAGAGGTGAAT	210	L31889
	Reverse	CCGTGTCGATTCGGATAAA		
GDNF	Forward	ACGGCCATACACCTCAATGT	144	GU229658
	Reverse	CCGTCTGTTTTTGGACAGGT		

BDNF, brain-derived neurotrophic factor; GDNF, glial cell line-derived neurotrophic factor; NGF, nerve growth factor; VEGF, vascular endothelial growth factor.

and contralateral group, $n=3$), each five sections at every 120- μm were stained with doublecortin, NeuN, RECA1, and cleaved caspase-3. The microscopic images were scanned and five typical frames (0.49 mm^2) were measured for each section. Thus, 75 frames on an average were determined per group. The positively stained area relative to total area (7.41 mm^2) was statistically analyzed using a Dynamic cell count, BZ-HIC (Keyence).

Real-time reverse transcription-polymerase chain reaction

Total RNA on cryosamples was extracted using Trizol (Invitrogen) from the area of the DiI-positive cells observed in the section. First-strand cDNA syntheses were performed from total RNA by reverse transcription with ReverTra Ace- α (Toyobo). Real-time reverse transcription-polymerase chain reaction (RT-PCR) amplifications were performed at 95°C for 10 s, at 62°C for 15 s, and at 72°C for 8 s using the porcine-specific primers *VEGF*. The specificity of the primers to porcine was confirmed by no amplification of the first-strand cDNA from rats with normal brains. The RT-PCR products were subcloned into a pGEM-T Easy vector (Promega) and confirmed by DNA sequencing based on published cDNA sequences. Gene expression of the transplanted cells in the infarct area was compared with that in the porcine normal brain tissue and that in transplanted cells in the normal brain after normalizing with β -actin.

In situ hybridization

Neurotrophic factors expressed in CD31⁻/CD146⁻ SP cells were examined with *in situ* hybridization in cryosections on day 21. Porcine cDNA of *VEGF* (224 bp), glial cell line-derived neurotrophic factor (*GDNF*; 144 bp), brain-derived neurotrophic factor (*BDNF*; 180 bp), and nerve growth factor (*NGF*; 210 bp) were linearized with *NcoI*, *SpeI*, *NcoI*, and *SpeI*, respectively, for anti-sense probes, and linearized with *SpeI*, *NcoI*, *SpeI*, and *NcoI*, respectively, for sense probes. The *VEGF* probe was constructed from plasmids after subcloning the PCR products using the same primers designed for real-time RT-PCR. The *GDNF*, *BDNF*, and *NGF* probes were also constructed in same way as the *VEGF* probe. Since

a published porcine *GDNF* sequence was not available, human primers for *GDNF* (forward 5'-TATGGGATGTCGTGGCTGT-3', reverse 5'-TCCACACCTTTTAGCGGAAT-3') were used for cDNA subcloning of porcine *GDNF* (630 bp). The design of the oligonucleotide primers (Table 1) was based on both published porcine cDNA sequences and the newly cloned cDNA sequence of the porcine *GDNF*. The four probes were labeled with DIG (Invitrogen) and the DIG signals were detected with TSA system FITC-conjugated tyramide (Invitrogen).

Migration, proliferation, and anti-apoptotic assays

At 50% confluence, the culture medium was switched to serum-free EBM-2. The conditioned medium (CM) from CD31⁻/CD146⁻ SP cells, CD31⁺/CD146⁻ SP cells, and unfractionated pulp cells were collected after 48 h.

For migration assay, modified Boyden chamber assays were performed with polyethylene terephthalate membrane (BD Bioscience) in a 24-well plate (BD Bioscience). SHSY5Y cells (Sanyo Chemical Industries, Ltd.) (1×10^5 cells/well) were seeded on the insert polyethylene terephthalate membrane, and 500 μL of DMEM-F12 (Sigma) with 20% of the three CMs was, respectively, poured into the tissue culture 24-well plate. SHSY5Y cells were derived from a neural crest tumor of early childhood, predominantly composed of undifferentiated neuroblast-like cells.⁷ After 24 h, the SHSY5Y cells passing through the membrane were counted after detaching them with 0.05% trypsin-0.02% EDTA.

For cell proliferation assay, SHSY5Y cells (1×10^3 /96-well plate) were cultured in DMEM-F12 containing 10% FBS for 24 h, and subsequently in serum-free DMEM-F12 containing 0.2% bovine serum albumin for further 24 h. Then, the medium was changed into each DMEM-F12 containing 0.02% FBS with 20% of three CMs. Ten micrometers of Tetra-color one (Seikagaku Kogyo, Co.) was added to the 96 well-plate, and cell numbers were measured by spectrophotometry at 450 nm at 2, 12, 24, 36, and 48 h of culture.

For the anti-apoptotic assay, SHSY5Y cells were cultured in DMEM-F12 in a 35-mm dish for 2 days and then incubated with 300 nM staurosporine⁸ (Sigma) in DMEM-F12 with 20% of the three CMs. After 24 h, SHSY5Y were harvested, and

the cell suspensions were treated with Annexin V-FITC (Roche Diagnostics) and PI for 15 min, and analyzed by flow cytometry JSAN.

BDNF (Peprotech), GDNF (Peprotech), VEGF-A (Peprotech), or NGF (Peprotech) at 50 ng/mL was used as a control for the three assays.

Evaluation of motor disability

Rats were blindly examined on days 0, 2, 6, and 9 with a standardized motor disability scale by slight modifications.⁹ Rats were scored 1 point for each of the following parameters: flexion of the forelimb contralateral to the stroke when instantly hung by the tail, extension of the contralateral hind limb when pulled from the table, and rotation to the paretic side against resistance. In addition, 1 point was scored for circling motion to the paretic side when trying to walk, 1 point was scored for failure to walk out of a circle of 50 cm in diameter within 10 s, 2 points were scored for failure to leave the circle within 20 s, and 3 points were scored for inability to exit the circle within 60 s. In addition, 1 point each was

scored for inability of the rat to extend the paretic forepaw when pushed against the table from above, laterally, and sideways. The motor disability scale was performed 3 times per animal time-point.

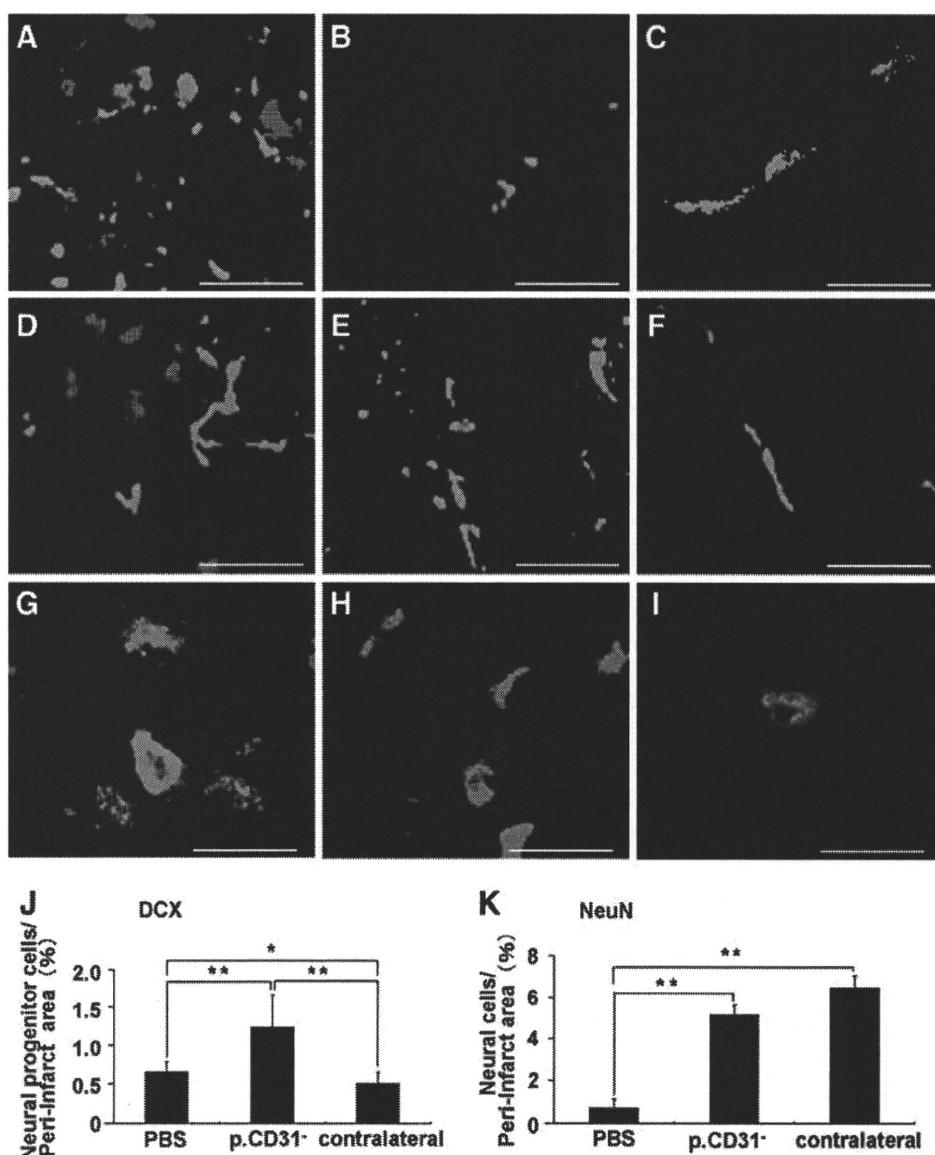
Assessment of infarct volume

The cryosections obtained from samples on days 3 and 21 were stained with hematoxylin and eosin.¹⁰ ImageJ (National Institutes of Health) was used to determine each infarct area in 9 coronal sections in 12- μ m thickness at 0.84-mm intervals. All of the infarction area was covered by these nine coronal sections. Regional infarct volumes were calculated by summing the infarct areas and multiplying these areas by the distance between sections (0.84 mm), followed by remediation for brain edema.¹¹

Statistical analyses

Data are reported as means \pm SD. *p*-Values were calculated using the unpaired Student's *t*-test.

FIG. 2. Doublecortin-positive cells (green: A–C), Neurofilament-positive cells (green: D–F), and NeuN-positive cells (green: G–I). CD31⁻/CD146⁻ SP cells (red) transplantation group of the ipsilateral (A, D, G) and the contralateral (B, E, H) on day 21. PBS group (C, F, I) on day 21. Statistical analyses of density of NPCs (J) and neurons (K) on day 21. Scale bars = 20 μ m. **p* < 0.005, ***p* < 0.001, Student's *t*-test. Each point is expressed as mean \pm SD of 75 determinations. NPC, neuronal progenitor cells; PBS, phosphate-buffered saline. Color images available online at www.liebertonline.com/tea



Results

Pulp stem cell outcome

DiI-labeled transplanted CD31⁻/CD146⁻ SP cells were characterized by round-to-oval nuclei with minimal variable cytoplasm. The transplanted cells survived and migrated from the original injection site to peri-infarct area in the cortex and striatum (Fig. 1D).

Transplanted cells localized in proximity of doublecortin (Fig. 2A) and neurofilament (Fig. 2D) or NeuN-positive cells (Fig. 2G) on day 21. Few doublecortin cells were observed in

the contralateral side (Fig. 2B). There was a twofold increase in doublecortin-positive cells (Fig. 2J) and an eightfold increase in NeuN-positive cells (Fig. 2K) on day 21 in the CD31⁻/CD146⁻ SP cell transplantation group compared with that in the PBS group. No evidence of differentiation of CD31⁻/CD146⁻ SP cells into neurons or endothelial cells was detected. The migration of NPCs with doublecortin from SVZ to the peri-infarct area was observed on days 9 and 21. The migration on day 9 was more prominent (Fig. 3I, K, M). These results suggest that the transplanted cells support the migration and differentiation of the NPCs. The number of

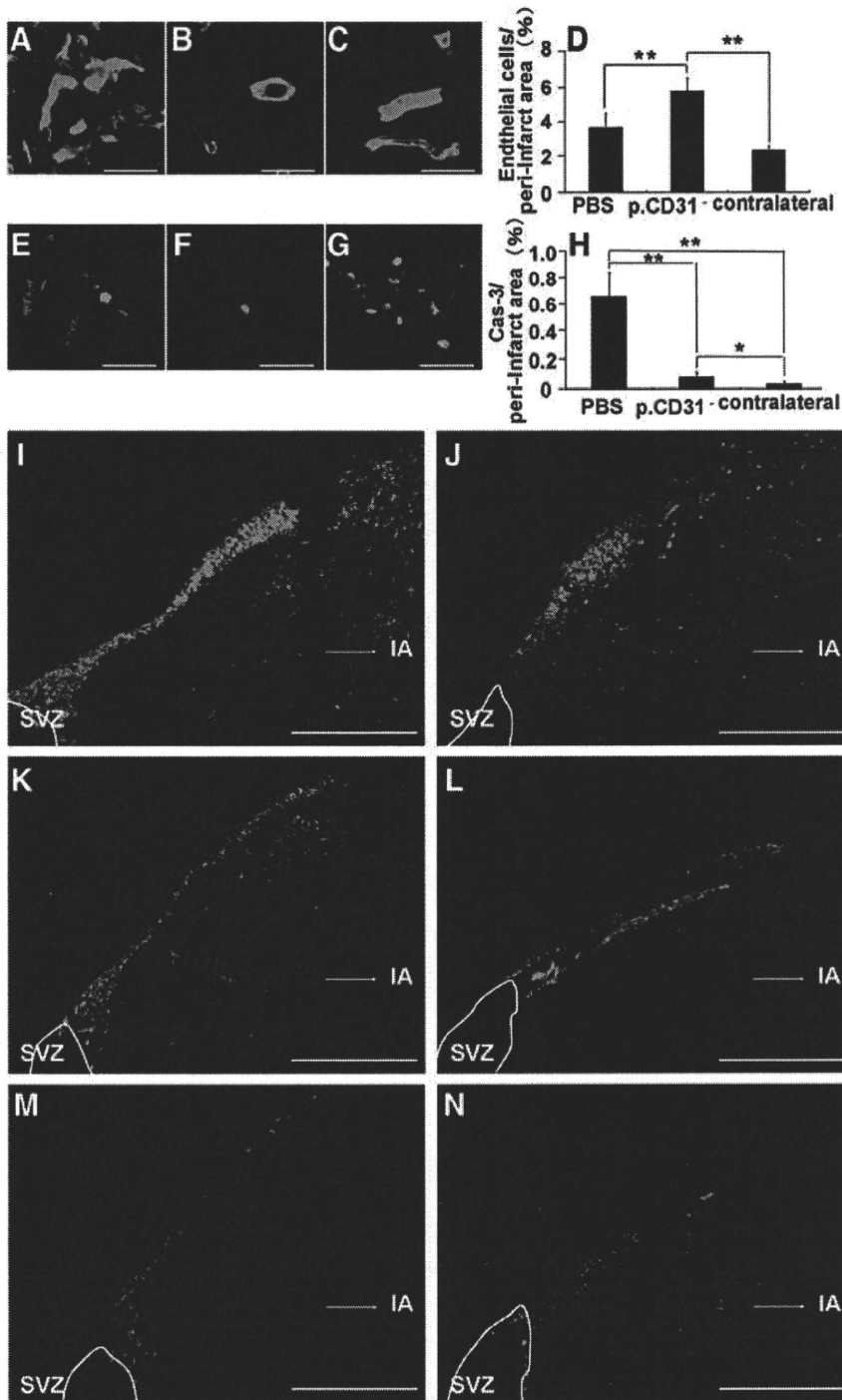


FIG. 3. RECA1-positive cells on day 21 (green: A–C) and cleaved caspase-3-positive cells on day 3 (green: E–G). CD31⁻/CD146⁻ SP cells (red) transplantation group of the ipsilateral (A, E) and the contralateral (B, F). PBS group (C, G). Statistical analyses of density of endothelial cells on day 21 (D) and cleaved caspase-3-positive cell on day 3 (H). The migration of NPC from the SVZ to the peri-infarct area on days 9 (I, J, M) and 21 (K, L, N). CD31⁻/CD146⁻ SP cells group (I, J). Unfractionated pulp cells (K, L). PBS group (M, N). Scale bar = 20 μm (A–C, E–G), and 300 μm (I–N). **p* < 0.01, ***p* < 0.001. Data were expressed as means ± SD at 75 determinations. The statistical difference was calculated by Student's *t*-test. IA, infarct area; SVZ, subventricular zone. Color images available online at www.liebertonline.com/tea

RECA1-positive cells on day 21 was increased in the CD31⁻/CD146⁻ SP cell transplantation group compared with that in the PBS group (Fig. 3D), indicating that the transplanted cells also promote angiogenesis after ischemia. In the CD31⁻/CD146⁻ SP cell transplantation group (Fig. 3H), there was a decrease in cleaved caspase-3-positive cells, suggesting that the transplanted cells have an anti-apoptotic function.

Expression of neurotrophic factors

The expression of several neurotrophic factors *VEGF*, *GDNF*, *NGF*, and *BDNF* was detected with *in situ* hybrid-

ization in the DiI-labeled CD31⁻/CD146⁻ SP cells in the peri-infarct area on day 21 (Fig. 4A–D). Real-time RT-PCR analysis demonstrated that expression of *VEGF* mRNA by the transplanted CD31⁻/CD146⁻ SP cells in the ischemic region on day 21 was 1,000 times and 28 times higher than that of normal porcine brain and that of the transplanted CD31⁻/CD146⁻ SP cells into normal rat striatum, respectively (Fig. 4E, F). Immunohistochemistry of *VEGF* showed that the *VEGF* protein was highly expressed in the DiI-labeled CD31⁻/CD146⁻ SP cells in the peri-infarct area on day 3 (Fig. 4G) compared with that on day 21 (Fig. 4H).

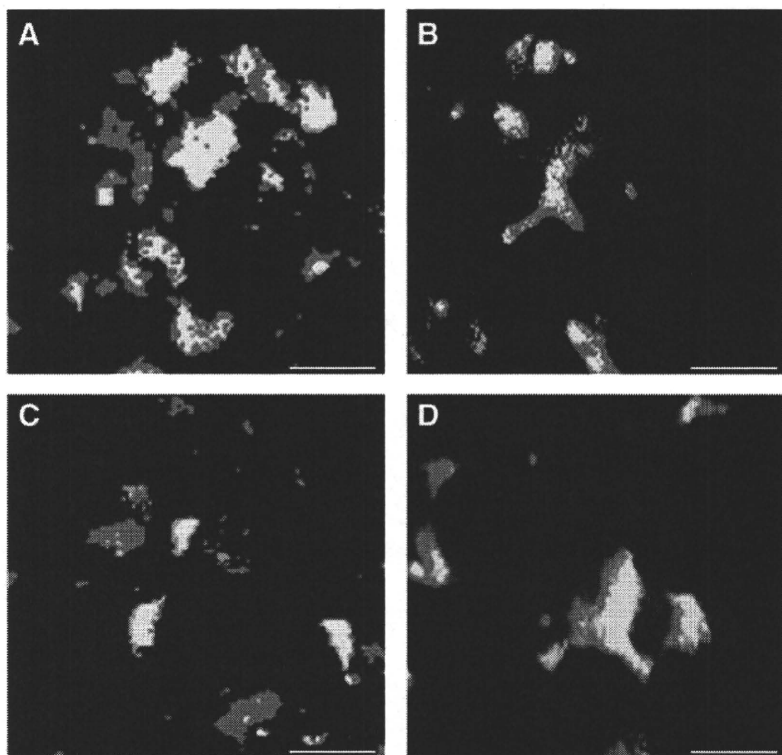
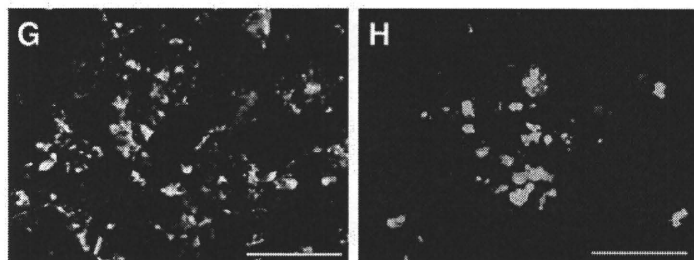
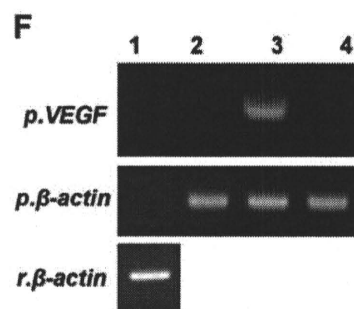
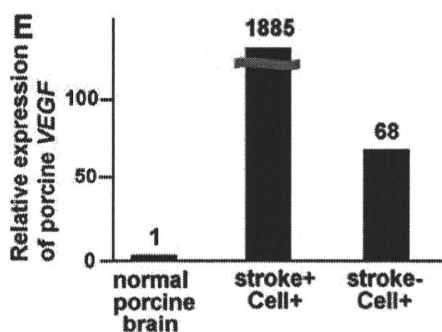


FIG. 4. Analysis of expression of *VEGF* (A), *GDNF* (B), *BDNF* (C), and *NGF* (D) (green: A–D) of DiI-labeled transplanted CD31⁻/CD146⁻ SP cells (red) by *in situ* hybridization in the peri-infarct area. Real-time reverse transcription–polymerase chain reaction analysis of porcine *VEGF* (*pVEGF*) using porcine-specific primers (E). Expression of porcine *VEGF* and porcine-specific and rat-specific β -actin 1, normal rat brain; 2, normal porcine brain; 3, peri-infarct area 21 days after transplantation of CD31⁻/CD146⁻ SP cells; 4, normal rat striatum 21 days after transplantation of the cells (F). *VEGF*-positive cells on day 3 (G) and on day 21 (H) by immunohistochemistry. Scale bars = 10 μ m (A–D) and 100 μ m (G, H). *BDNF*, brain-derived neurotrophic factor; *GDNF*, glial cell line-derived neurotrophic factor; *NGF*, nerve growth factor; *VEGF*, vascular endothelial growth factor. Color images available online at www.liebertonline.com/tea



Migration, proliferation, and anti-apoptotic assays

CM of CD31⁻/CD146⁻ SP cells showed higher migratory effect on SHSY5Y cells than VEGF, NGF, and BDNF, and was similar to GDNF (Fig. 5A). Its proliferation effect was higher than VEGF and NGF, and similar to BDNF and GDNF (Fig. 5B). Its anti-apoptotic activity was higher than BDNF, GDNF, and VEGF (Fig. 5C).

Evaluation of motor function

All groups (CD31⁻/CD146⁻ SP cells, unfractionated pulp cells, and PBS) displayed high score for motor function at the early stage (day 0, scores are 8.08±0.79; 8.25±0.96; 8.42±0.79, and day 2, 5.08±0.90; 6.25±1.26; 7.67±0.78, respectively). Progressive improvement in motor disability in the CD31⁻/CD146⁻ SP cell transplantation group after day 2 became significant on day 6 compared with PBS control group (2.67±1.23; 6.83±0.72), and more significant on day 9 compared with the unfractionated pulp cells and the PBS control group (1.33±0.78; 2.8±0.96; 6.50±0.67) (Fig. 6A). Persistent improvement in CD31⁻/CD146⁻ SP cells trans-

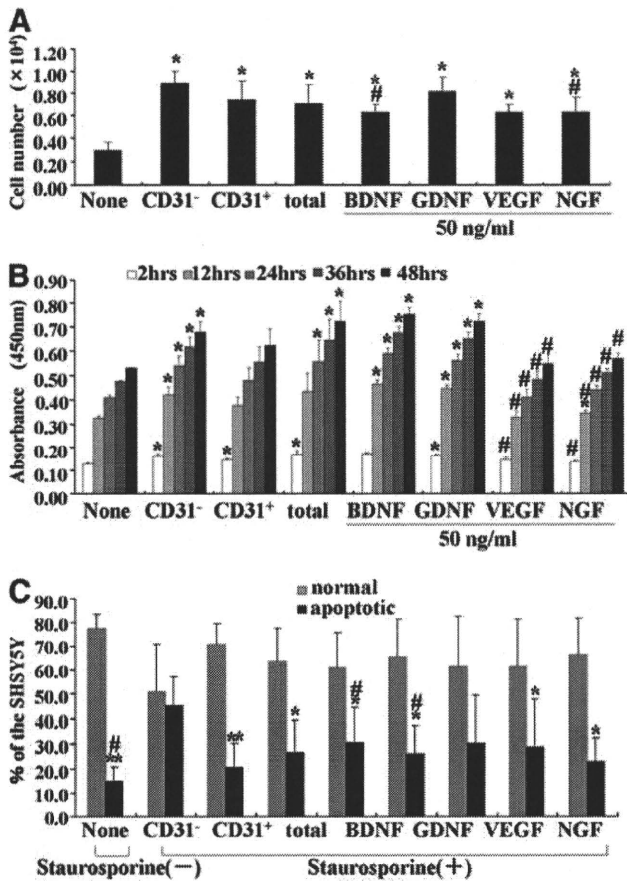


FIG. 5. The migration (A), proliferative effect (B), and anti-apoptotic effect (C) of conditioned medium of CD31⁻/CD146⁻ SP cells, CD31⁺/CD146⁻ SP cells, and unfractionated total pulp cells and neurotrophic factors on SHSY5Y cells. **p*<0.05, ***p*<0.005, versus control. #*p*<0.05, versus CD31⁻/CD146⁻ SP cells. Data were expressed as means±SD at three determinations (A, C) and four determinations (B). Student's *t*-test.

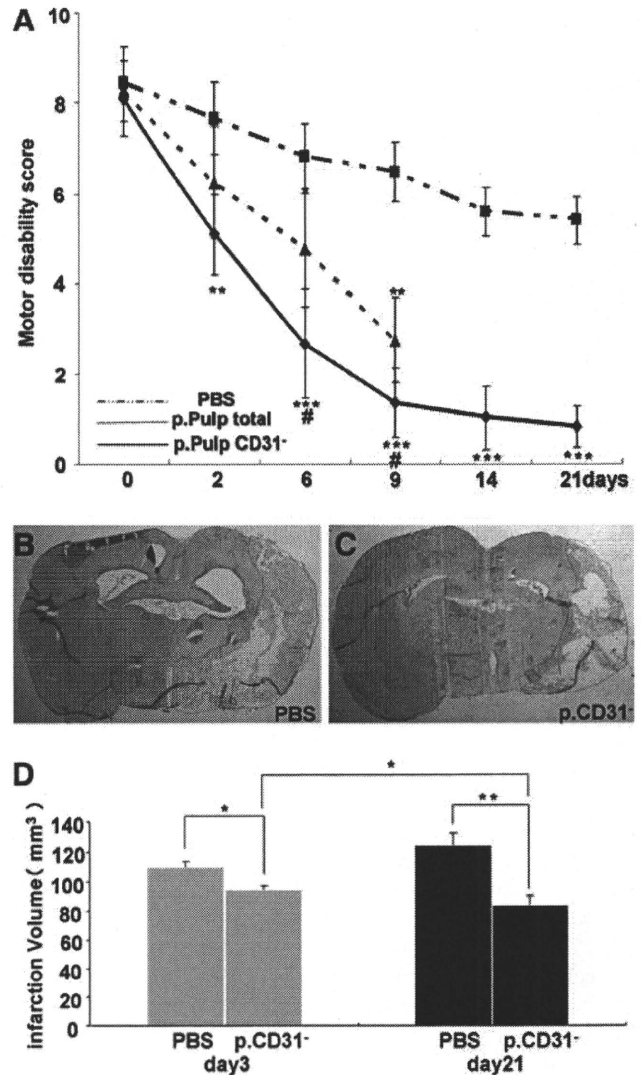


FIG. 6. Motor disability test by injection of the CD31⁻/CD146⁻ SP cells, the unfractionated pulp cells and the PBS on days 0, 2, 6, and 9 (A). Infarct area on day 21 (B, C). The reduction of the infarct volume 3 and 21 days after injection of CD31⁻/CD146⁻ SP cells (D). **p*<0.05, ***p*<0.005, ****p*<0.001, versus control. #*p*<0.05, versus CD31⁻/CD146⁻ SP cells. Data were expressed as means±SD at three determinations (D), Student's *t*-test.

plantation group was noted on day 14 (1.00±0.71) and 21 (0.80±0.45), whereas persistent impairment of motor disability (score above 4) was observed in the PBS group on day 14 (5.60±0.55) and 21 (5.40±0.59) (Fig. 6A). Further, the video image demonstrated significant recovery in motor function of the CD31⁻/CD146⁻ SP cell transplantation group compared with the unfractionated pulp cells and PBS control groups on day 6 (Supplementary Videos S1–S3; Supplementary Data are available online at www.liebertonline.com/tea).

Reduction of infarct volume

There was a significant decrease in the infarct volume on days 3 and 21 in the CD31⁻/CD146⁻ SP cell transplantation

group (day 3, $95.2 \pm 2.5 \text{ mm}^3$, $n=3$; day 21, $84.7 \pm 6.5 \text{ mm}^3$, $n=4$) compared to PBS group (day 3, $109.7 \pm 4.1 \text{ mm}^3$, $n=3$; day 21, $123.9 \pm 7.4 \text{ mm}^3$, $n=4$). The difference of infarct volume between the CD31⁻/CD146⁻ SP cell transplantation group and the PBS group increased over time (reduced by 13.3% on day 3 and reduced by 32.9% on day 21) (Fig. 6D). These results suggest that transplanted CD31⁻/CD146⁻ SP cells promoted the regeneration.

Discussion

In the current study, we demonstrated that transplanted CD31⁻/CD146⁻ SP cells migrated to the peri-infarct area. In addition, these cells released neurotrophic factors, and promoted migration and differentiation of the endogenous NPCs in SVZ. They also induced vasculogenesis in the peri-infarct area. These results indicate that CD31⁻/CD146⁻ SP cells ameliorated the ischemic tissue injury and accelerated the functional recovery after TMCAO. We have hypothesized that three mechanisms may contribute to the actions of VEGF. First, VEGF produced by transplanted cells may promote neurogenesis. NPCs in SVZ are known to migrate to the peri-infarct area and differentiate into neurons.¹ In this study, VEGF induced a chemotactic response in SHSY5Y cells. The transplanted CD31⁻/CD146⁻ SP cells migrated to the peri-infarct area and expressed VEGF. These results suggest that VEGF released by CD31⁻/CD146⁻ SP cells in the peri-infarct area may promote migration of the endogenous NPCs in SVZ. Second, VEGF produced by transplanted cells may promote vasculogenesis. VEGF binds to its receptors on locally present vascular endothelial cells and directly initiates the angiogenic response.¹² In this study, the number of RECA1-positive endothelial cells significantly increased in the cell transplantation group. Third, VEGF may provide a neuroprotective effect. The neuroprotective effects of VEGF in experimental cerebral ischemia have been reported.¹³ In cell the transplantation group, the number of cleaved caspase-3-immunopositive cells in the peri-infarct area was decreased compared with that in the PBS group, thus demonstrating the anti-apoptotic effects of VEGF on SHSY5Y cells. These results suggest that VEGF produced by CD31⁻/CD146⁻ SP cells may inhibit apoptosis of neurons. Thus, VEGF demonstrates pleiotropic effects on neurogenesis, vasculogenesis, and neuroprotection.

As VEGF is a potent vascular permeability factor, it may accelerate brain edema after stroke. Administration of VEGF in early ischemia (1 h after ischemia) leads to significant increase in blood-brain barrier leakage as well as enlarged ischemic areas.¹⁴ However, VEGF administration at 24 h after TMCAO reduces infarct size, improves neurologic recovery, enhances neurogenesis in the SVZ and angiogenesis in the ischemic border zone.¹⁴ In this study, CD31⁻/CD146⁻ SP cells were transplanted 24 h after TMCAO and we monitored the reduction of infarct size and improvement of motor disability. The time of administration of cells is critical. Thus, if CD31⁻/CD146⁻ SP cells were transplanted during an optimal window of time, they exhibit beneficial effects without the deleterious effects of edema.

In addition, CD31⁻/CD146⁻ SP cells expressed other neurotrophic factors such as GDNF,¹⁵ NGF,¹⁶ and BDNF¹⁶ in the peri-infarct area. These neurotrophic factors had migratory, proliferative, and/or anti-apoptotic effects on SHSY5Y

cells *in vitro* and may also contribute to the recovery from ischemic brain injury.

Finally, we explored the plausible underlying mechanisms of how injection of CD31⁻/CD146⁻ SP cells into the brains of immunocompetent rats staved off graft rejection. Blood-brain barrier is known to play a critical role in maintaining the immune-privileged status of the central nervous system.¹⁷ It is well known that mesenchymal stem cells from bone marrow are not rejected by hosts and immunosuppression is not required in rodents.¹ Dental pulp stem cells have many similarities to mesenchymal stem cells; transplanted CD31⁻/CD146⁻ SP cells possess immunosuppressive properties.¹⁸

Conclusion

In summary, the transplantation of porcine CD31⁻/CD146⁻ SP cells promotes neurogenesis and vasculogenesis in an induced peri-infarct area, and enhances recovery after TMCAO in rats. Further research is needed to understand the underlying mechanisms. For potential clinical application and translational studies, the safety of CD31⁻/CD146⁻ SP cells must be assessed, including tumor formation. In conclusion, regeneration therapy using CD31⁻/CD146⁻ SP cells is a potential candidate in the treatment of stroke.

Acknowledgments

The authors thank Drs. Masataka Ito, Kayo Adachi, and Kiyomi Imabayasghi for their assistance. This work was supported by funds from Collaborative Development of Innovative Seeds, Potentiality verification stage from Japan Science and Technology Agency, a Grant-in-Aid for Scientific Research from the Ministry of Education, Science, Sports and Culture, Japan, No. 19659499 (M.N.), No. 20390504 (M.N.), and No. 18592173 (H.H.), and the Research Grant for Longevity Sciences (19C-2, 21A-7) from the Ministry of Health, Labour, and Welfare (M.N.).

Disclosure Statement

No competing financial interests exist.

References

1. Burns, T.C., Verfaillie C.M., and Low W.C. Stem cells for ischemic brain injury: a critical review. *J Comp Neurol* **515**, 125, 2009.
2. Locatelli, F., Bersano, A., Ballabio, E., Lanfranconi, S., Papadimitriou, D., Strazzer, S., Bresolin, N., Comi, G.P., and Corti, S. Stem cell therapy in stroke. *Cell Mol Life Sci* **66**, 757, 2009.
3. Gage, F.H., Kempermann, G., Palmer, T.D., Peterson, D.A., and Ray, J. Multipotent progenitor cells in the adult dentate gyrus. *J Neurobiol* **36**, 249, 1998.
4. Yang, K.L., Chen, M.F., Liao, C.H., Pang, C.Y., and Lin, P.Y. A simple and efficient method for generating Nurr1-positive neuronal stem cells from human wisdom teeth (tNSC) and the potential of tNSC for stroke therapy. *Cytotherapy* **11**, 606, 2009.
5. Iohara, K., Zheng, L., Wake, H., Ito, M., Nabekura, J., Wakita, H., Nakamura, H., Into, T., Matsushita, K., and Nakashima, M. A novel stem cell source for vasculogenesis in ischemia: subfraction of side population cells from dental pulp. *Stem Cells* **26**, 2408, 2008.

6. Longa, E.Z., Weinstein, P.R., Carlson, S., and Cummins, R. Reversible middle cerebral artery occlusion without craniectomy in rats. *Stroke* **20**, 84, 1989.
7. Koning, G., Colin, L., and Beyreuther, K. Retionic acid induced differentiated neuroblastoma cells show increased expression of the β A4 amyloid gene of Alzheimer's disease and an altered splicing pattern. *FEBS Lett* **269**, 305, 1990.
8. Richard, B., Eric, S., Patrick, O., Kurt, W., and Ywes, P. Induction of a common pathway of apoptosis by staurosporine. *Exp Cell Res* **211**, 314, 1994.
9. Leker, R.R., Gai, N., Mechoulam, R., and Ovadia, H. Drug-induced hypothermia reduces ischemic damage: effects of the cannabinoid HU-210. *Stroke* **34**, 2000, 2003.
10. Ginsberg, M.D. Adventures in the pathophysiology of brain ischemia: penumbra, gene expression, neuroprotection: the 2002 Thomas Willis Lecture. *Stroke* **34**, 214, 2003.
11. Leach, M.J., Swan, J.H., Eisenthal, D., Dopson, M., and Nobbs, M. BW619C89, a glutamate release inhibitor, protects against focal cerebral ischemic damage. *Stroke* **24**, 1063, 1993.
12. Plate, K.H., Beck, H., Danner, S., Allegrini, P.R., and Wiessner, C. Cell type specific upregulation of vascular endothelial growth factor in an MCA-occlusion model of cerebral infarct. *J Neuropathol Exp Neurol* **58**, 654, 1999.
13. Jin, K.L., Mao, X.O., and Greenberg, D.A. Vascular endothelial growth factor: direct neuroprotective effect in *in vitro* ischemia. *Proc Natl Acad Sci U S A* **97**, 10242, 2000.
14. Heike, B., and Karl, H.P. Angiogenesis after cerebral ischemia. *Acta Neuropathol* **117**, 481, 2009.
15. Leu-Fen, H., Lin, H., Doherty, D., Lile, B., and Frank, C. GDNF: a glial cell line-derived neurotrophic factor for midbrain dopaminergic neurons. *Science* **260**, 1072, 1993.
16. Shawne, N., Fernando, G., James, C., and Carl, C. Physical activity increases mRNA for brain-derived neurotrophic factor and nerve growth factor in rat brain. *Brain Res* **726**, 49, 1996.
17. Pachter, J.S., De Vries, H.E., and Fabry, Z. The blood-brain barrier and its role in immune privilege in the central nervous system. *J Neuropathol Exp Neurol* **62**, 593, 2003.
18. Pierdomenico, L., Bonsi, L., Calvitti, M., Rondelli, D., Arpinati, M., Chirumbolo, G., Becchetti, E., Marchionni, C., Alviano, F., Fossati, V., Staffolani, N., Franchina, M., Grossi, A., and Bagnara, G.P. Multipotent mesenchymal stem cells with immunosuppressive activity can be easily isolated from dental pulp. *Transplantation* **80**, 836, 2005.

Address correspondence to:

Misako Nakashima, Ph.D.

Department of Oral Disease Research

National Center for Geriatrics and Gerontology

Research Institute

35 Gengo, Morioka, Obu

Aichi 474-8522

Japan

E-mail: misako@ncgg.go.jp

Received: May 24, 2010

Accepted: January 10, 2011

Online Publication Date: February 22, 2011

Complete pulp regeneration after pulpectomy by transplantation of CD105⁺ stem cells with SDF-1

Koichiro Iohara,¹ Kiyomi Imabayashi,¹ Ryo Ishizaka,^{1,2} Atsushi Watanabe,³
Junichi Nabekura,⁴ Masataka Ito,⁵ Kenji Matsushita,¹ Hiroshi Nakamura,⁶ and
Misako Nakashima^{1,*}

¹Department of Oral Disease Research, National Center for Geriatrics and Gerontology, Research Institute, 35 Gengo, Morioka, Obu, Aichi 474-8522, Japan

²Department of Pediatric Dentistry, School of Dentistry, Aichi-gakuin University, Nagoya, Aichi 464-8651, Japan

³Department of Cognitive Brain Science, National Center for Geriatrics and Gerontology, Research Institute, Obu, Aichi 474-8522, Japan

⁴Department of Developmental Physiology, National Institute for Physiological Sciences, Okazaki, Aichi 444-8585, Japan

⁵Department of Developmental Anatomy and Regenerative Medicine, National Defense Medical College, Tokorozawa, Saitama 359-8513, Japan

⁶Department of Endodontology, School of Dentistry, Aichigakuin University, Nagoya, Aichi 464-8651, Japan

*Correspondence: Misako Nakashima, Ph.D. Department of Oral Disease Research, National Center for Geriatrics and Gerontology, Research Institute, 35 Gengo, Morioka, Obu, Aichi 474-8522, Japan, E-mail: misako@ncgg.go.jp

Key words Dental pulp progenitor/stem cells · autologous cell transplantation · CD105 · pulp regeneration · stromal cell-derived factor-1 · pulpectomy

Abbreviations RT-PCR, reverse transcription-polymerase chain reaction, Dspp, dentin sialophosphoprotein, SDF-1, stromal cell-derived factor-1

Running Title: Pulp regeneration with dental pulp stem cells.

ABSTRACT

Loss of pulp due to caries and pulpitis leads to loss of teeth and reduced quality of life. Thus there is an unmet need for regeneration of pulp. A promising approach is stem cell therapy. Autologous pulp stem/progenitor (CD105⁺) cells were transplanted into a root canal with stromal cell-derived factor (SDF)-1 following pulpectomy in mature teeth with complete apical closure in dogs. The root canal was successfully filled with regenerated pulp including nerves and vasculature by day 14, followed by new dentin formation along the dentinal wall. The newly regenerated tissue was significantly larger in the transplantation of pulp CD105⁺ cells with SDF-1 compared with those of adipose CD105⁺ cells with SDF-1 or unfractionated total pulp cells with SDF-1. The pulp CD105⁺ cells highly expressed angiogenic/neurotrophic factors compared to other cells, and localized in the vicinity of newly formed capillaries after transplantation, demonstrating its potent trophic effects on neovascularization. Two dimensional electrophoretic analyses and real-time RT-PCR analyses demonstrated that the qualitative and quantitative protein and mRNA expression patterns of the regenerated pulp were similar to those of normal pulp. Thus, this novel stem cell therapy is the first demonstration of complete pulp regeneration, implying novel treatment to preserve and save teeth.

INTRODUCTION

~~Dental caries and pulp inflammation are common afflictions of teeth. Deep caries and pulp exposure have been treated by pulp capping or pulp amputation to conserve pulp tissue, with limited success, leading to early loss of dental pulp and further resultant loss of the tooth due to tooth fracture and/or periapical disease.~~ Dental pulp has many functions, and is essential for longevity of teeth and quality of life. The long term goal of endodontic treatment

following deep caries and/or pulp inflammation is the conservation and restoration of teeth including dental pulp. A promising approach for it is stem cell based therapy to regenerate the dentin-pulp complex for the conservation and total restoration of structure and function¹. The regeneration and tissue engineering of pulp is based on morphogens and growth factors, responding stem/progenitor cells and the extracellular matrix scaffold². The regeneration of dental pulp in immature teeth with incomplete apical closure has been reported using fibrin in the blood clot or collagen^{3,4}. However, there have been no reports concerning total pulp regeneration in mature teeth with complete apical closure by stem/progenitor cell therapy. There is an intimate association of innervation with vasculature of the dental pulp. Angiogenesis/vasculogenesis and neurogenesis are critical for total functional pulp regeneration. ~~SDF-1 is implicated as a chemokine for CXCR4 positive stem cells, and~~ The type III receptor of the transforming growth factor (TGF)- β receptor family cell surface antigen CD105 (endoglin) was selected on the basis of its wide expression on mesenchymal stem cells⁵. The SDF-1/CXCR4 axis is present and functional in MSC populations^{6,7}. CD105⁺ stem/progenitor cells from human pulp tissue containing CXCR4-positive cells demonstrated angiogenic/vasculogenic and neurogenic potential⁸. Endothelial cells release stromal cell-derived factor (SDF)-1 under hypoxic conditions and promote cell survival and neovascularization by recruitment and perivascular retention of CXCR4-positive bone marrow-derived cells^{9,10}. Therefore, in this study autologous pulp CD105⁺ cells were transplanted with SDF-1 in a collagen scaffold into the root canal of mature teeth induced complete apical closure after pulpectomy, in dogs. Thus, we demonstrate for the first time complete pulp regeneration in the root canal, by protein profiles and mRNA expression patterns.

MATERIALS AND METHODS

Cell Isolation. Dental pulp cells were separated from pulp tissues of maxillary teeth in dogs as described previously¹¹. Primary adipose cells were also separated from the adipose tissue of the same dog as a control. Those primary cells, $2\sim 5\times 10^5$ cells each were stained with anti-mouse IgG1 negative control (W3/25) (AbD Serotec Ltd., Oxford, UK), mouse IgG1 negative control (Phycoerythrin, PE) (MCA928PE) (AbD Serotec), and mouse anti-human CD105 (PE) (43A3) (BioLegend, San Diego, CA, USA), 10 μ l per 10^6 cells for 90 min at 4°C, and were sorted by a flow cytometer JSAN (Bay Bioscience, Kobe, Japan). CD105⁺ cells and CD105⁻ cells both derived from the pulp and adipose tissue and total pulp cells without cell fractionation were cultured in EBM2 (Cambrex Bio Science, Walkersville, Maryland, USA) supplemented with 10 ng/ml IGF (Cambrex Bio Science), 5 ng/ml EGF (Cambrex Bio Science) and 10% FBS (Invitrogen Corporation, Carlsbad, CA, USA) to maintain the cells. They were subcultured after reaching 60-70% confluence.

The phenotype of pulp CD105⁺ cells was further characterized by flowcytometry at the third passage of culture in comparison with adipose CD105⁺ cells and unfractionated total pulp cells after immunolabeling with antigen surface markers (SI M&M). The experiments were repeated nine times.

Real-Time Reverse Transcription-Polymerase Chain Reaction Analysis

To further characterize the phenotype of the cell populations total RNA were extracted using Trizol (Invitrogen) from the pulp and adipose CD105⁺ cells and total pulp cells at the third passage. The number of these cells was normalized to 5×10^4 cells in each experiment. First-strand cDNA syntheses were performed from total RNA by reverse transcription using the ReverTra Ace- α (Toyobo, Tokyo, Japan). Real time RT-PCR amplifications were performed at 95°C for 10 sec, 62°C for 15 sec, 72°C for 8 sec using stem cell markers, canine *CXCR4*, *Sox2*, *Stat3*, *Bmi1* and *Rex1* (Supplementary Table 1) labeled with Light Cycler-Fast

Start DNA master SYBR Green I (Roche Diagnostics, Pleasanton, CA) in Light Cycler (Roche Diagnostics). The design of the oligonucleotide primers was based on published canine cDNA sequences. When canine sequences were not available, human sequences was used. To examine mRNA expression of angiogenic and neurotrophic factors, real-time RT-PCR amplifications of canine *matrix metalloproteinase (MMP)-3*, *VEGF-A*, *granulocyte-monocyte colony-stimulating factor (GM-CSF)*, *SDF-1*, *NGF*, *BDNF*, *Neuropeptide Y*, *Neurotrophin 3*, *E-selectin*, *VCAM 1*, *rhombotin 2*, *ECSCR* and *SLC6A6* were also performed (Supplementary Table 1). The RT-PCR products were confirmed by sequencing based on published cDNA sequences. The expression in pulp CD105⁺ cells and adipose CD105⁺ cells was compared with that in total pulp cells at the third passage of culture after normalizing with *β-actin*.

Induced Differentiation

The differentiation of pulp CD105⁺ cells from the third to fifth passage, into adipogenic, angiogenic, neurogenic, odontogenic/osteogenic lineages was determined and compared with adipose CD105⁺ cells and unfractionated pulp cells as described previously¹².

Proliferation and Migration Assay

To determine cell proliferation in response to stromal cell-derived factor-1 (SDF1) (Acris, Herford, Germany), pulp CD105⁺ cells were compared with total pulp cells and adipose CD105⁺ cells at fourth passage at the 10³ cells per 96 well in EBM2 supplemented with 0.2% bovine serum albumin (Sigma) and SDF-1 (50 ng/ml). Ten μl of Tetra-color one[®] (Seikagaku Kogyo, Co., Tokyo, JAPAN) was added to the 96 well plate, and cell numbers were measured at 2, 12, 24, and 36 hours of culture using spectrophotometer at 450 nm absorbance. Wells without cells served as negative controls.

To examine migration activity of pulp CD105⁺ cells by SDF-1, horizontal chemotaxis assay was performed compared with total pulp cells and adipose CD105⁺ cells. The TAXIScan-FL (Effector Cell Institute, Tokyo, JAPAN) was used to detect real-time horizontal chemotaxis of cells. The TAXIScan-FL consists of an etched silicon substrate and a flat glass plate, both of which form two compartments with a 6 µm deep microchannel. Each cell fraction (1µl of 10⁵cells/ml) was placed into the single hole with which the device is held together with a stainless steel holder, and 1 µl of 10 ng/µl of SDF-1 was placed into the contra-hole. The video images of cell migration were taken for 6 hours.

In Vivo Transplantation Studies

An experimental model of whole pulp removal and transplantation of cell populations for regeneration was established in the permanent teeth in dogs to achieve complete apical closure (Narc, Chiba, Japan). The whole pulp removal was carried out in the both side of upper second incisors and lower third incisors under intravenously administered sodium pentobarbital (Schering-Plough, Germany) followed by enlargement of apical foramen, 0.7 mm in width using #70 K-file (MANI Inc, Tochigi, Japan). Autologous transplantation of the pulp CD105⁺ cells, adipose CD105⁺ cells or total pulp cells, 1x10⁶cells in each, from the third to fourth passage, after DiI labeling was performed with collagen TE, a mixture of collagen type I and type III (Nitta Gelatin, Osaka, Japan) in the lower part of the root canals. The upper part of the root canals was further filled with SDF-1 at the final concentration of 15ng/µl, with collagen TE. The cavity was sealed with zinc phosphate cement (Elite Cement, GC, Tokyo, Japan) and composite resin (Clearfil FII, Kuraray, Kurashiki, Japan) following treatment with a bonding agent (Clearfil Mega Bond, Kuraray). Sixty teeth from 15 dogs were used. Ten teeth transplanted with pulp CD105⁺ cells with SDF-1, 5 teeth transplanted with adipose CD105⁺ cells with SDF-1, 5 teeth transplanted with total pulp cells with SDF-1,

5 teeth with SDF-1 only without cells, 5 teeth with pulp CD105⁺ cells only without SDF-1, and 5 teeth with a scaffold only without cells were harvested for histology after 14 days. Six teeth transplanted with pulp CD105⁺ cells with SDF-1 were harvested for two dimensional electrophoretic analyses after 28 days. Four teeth each transplanted with pulp CD105⁺ cells with SDF-1, adipose CD105⁺ cells with SDF-1 and total pulp cells with SDF-1 were harvested after 90 days, respectively. Seven normal teeth without any operation were used as control. For morphological analyses, they were fixed in 4% paraformaldehyde (PFA) (Nakarai Tesque, Kyoto, Japan) at 4°C overnight and embedded in paraffin wax (Sigma) after demineralization with 10% formic acid. The paraffin sections (5µm in thickness) were morphologically examined after staining with hematoxylin and eosin (HE).

All animal experiments were conducted using the strict guidelines of the Animal Protocol Committees and DNA Safety Programs both in National Center for Geriatrics and Gerontology and Aichigakuin University.

For vascular staining, 5-µm-thick paraffin sections stained with Fluorescein Griffonia (Bandeiraea) Simplicifolia Lectin 1/fluorescein-galanthus nivalis (snowdrop) lectin (20µg/ml, Vector laboratories, Inc., Youngstown, Ohio) for 15 min using a fluorescence microscope BIOREVO, BZ-9000 (KEYENCE, Osaka, Japan).

For whole mount staining of vascular structure, the regenerated tissue and normal pulp tissue were dissected from teeth on day 14, and fixed in 4% paraformaldehyde for 45min. The tissue was treated with 0.3% Triton X in PBS, blocked and stained with isolectin GS-IB4 from Griffonia simplicifolia, Alexa Fluor 488 conjugate (1:500) for 12 hours at 4°C overnight. Neovascularization and engraftment of the transplanted cells into the root canal was examined by two-photon microscopy using FV1000MPE (Olympus) instrument. Three dimensional structures were reconstructed by FV10-ASW software.

For neuronal staining, 5-µm-thick paraffin sections incubated for 15 min with 0.3% Triton

X-100 (Sigma Chemical; St Louis, MO). After incubation with 2.0% normal goat serum to block non-specific binding, they were incubated with goat anti-human PGP9.5 (Ultra Clone Ltd.) (1:10000) at 4°C overnight. After three washes in PBS, bound antibodies were reacted with biotinylated goat anti-rabbit IgG secondary antibody (Vector) (1:200) for 1 hour at room temperature. The sections were also developed with the ABC reagent (Vector Laboratories, Burlingame, CA), using the DAB chromogen for 10 min.

Relative amounts of regenerative pulp tissue 14 days after transplantation were examined in each sample by capturing video images of the histological preparations on the binocular microscopy (Leica, M 205 FA). Three sections at 150- μ m intervals for each tooth from a total of 5 teeth each transplanted with pulp CD105⁺ cells with SDF-1, adipose CD105⁺ cells with SDF-1, total pulp cells with SDF-1, pulp CD105⁺ cells only, SDF-1 only, and collagen TE scaffold only were examined. On-screen image outlines of newly regenerated pulp tissue and newly formed dentin were traced, and the surface area of these outlines in the root canal was determined by using Leica Application Suite software. The ratio of the regenerated area to the root canal area was calculated in three sections of each tooth and the mean value was determined.

In vivo gene expression of odontoblastic differentiation markers, *dentin sialophosphoprotein (Dsp)* and *enamelysin* in the cells lining along the root canal surface was examined by in situ hybridization in 5 μ m-paraffin sections 90 days after transplantation of pulp CD105⁺ cells with SDF-1. Canine cDNA of *Dsp* (183bp) and *enamelysin* (195bp) linearized with *Nco*I and *Spe*I, respectively, were used as anti-sense probes. The probes were constructed out of the plasmids after subcloning the PCR products using the same primers as these designed for real-time RT-PCR (Supplementary Table 1). The DIG signals were detected by TSA system (PerkinElmer, Waltham, MA, USA).

Two Dimensional Electrophoretic Analyses and Gene Expression Analyses

For two dimensional electrophoretic analysis, the regenerated pulp-like tissue on day 28, normal pulp, and periodontal ligament were homogenized in lysis buffer (6 M urea, 1.97 M thiourea, 2% (w/v) CHAPS, 64.8 mM DTT, 2% (v/v) Pharmalyte) and sonicated. The supernatant was collected after centrifuged at 15,000rpm for 15 min at 4°C, and applied to 2-dimensional electrophoresis. Isoelectric focusing (IEF) was carried out using CoolPhoreSter 2-DE systems. IPG strips (Immobiline DryStrips, pH 4-7, 18 cm, GE) were used according to manufacturer's instructions. IPG strips were rehydrated with rehydration solution (6 M urea, 1.97 M thiourea, 2% (v/v) TritonX-100, 13 mM DTT, 2% (v/v) Pharmalyte, 2.5 mM acetic acid, 0.0025% BPB) for overnight at 20°C. IEF was performed following a step wise voltage incremental manner: 500 V for 2 hours, 700-3000 V for 1hour, and 3500 V for 24 hours. After IEF, IPG strips were incubated in equilibration buffer (6M urea, 32.4 mM DTT, 5 mM Tris-HCl, pH 6.8, 2% (w/v) SDS, 0.0025% BPB, 30% (v/v) Glycerol) for 30 min. IPG strips were further equilibrated in 5 mM Tris-HCl, pH 6.8, 2% (w/v) SDS, 0.0025% BPB, 30% (v/v) Glycerol, 243 mM iodoacetamid for 20 min. Separation in the second dimension was carried out in 12.5% SDS-PAGE gels (20 cm × 20 cm) at a constant current of 25 mA/gel for 15 min and 30 mA/gel thereafter. The gels were stained with Flamingo Fluorescent Gel Stain (Bio-Rad Laboratories, CA, USA) and scanned (FluoroPhorester 3000, Anatech, Tokyo, Japan). The gel images were analyzed and compared each other by using Progenesis (Nonlinear Dynamics, NC, USA).

Real time RT-PCR amplifications were performed as previously described using markers for periodontal ligament, canine *axin2*, *periostin*, and *asporin/periodontal ligament-associated protein 1 (PLAP-1)*. *Collagen al(1)*, *syndecan3*, and *tenascin C* were also used for comparison of regenerated tissue with normal pulp and periodontal ligament (Supplementary Table 1).

For microarray analysis biotinylated cRNA were prepared from 250 ng of total RNA according to the standard Affymetrix protocol (Affymetrix Japan K.K., Tokyo, Japan). Following fragmentation, 10 μ g of cRNA were hybridized for 16 hours at 45°C on GeneChip Canine Genome 2.0 Array (Affymetrix) containing ~43,000 annotated sequences. GeneChips were washed and stained in the Affymetrix Fluidics Station 450, and were scanned using the Affymetrix GCS3000 scanner. The data were analyzed with Microarray Suite version 5.0 (MAS 5.0) using Affymetrix default analysis settings and global scaling as normalization method. The trimmed mean target intensity of each array was set to 500. Chips were ordered into hierarchical clusters using the Pearson centered algorithm as the distance measure, and the Average algorithm as the linkage method.

Statistical Analyses

Data are reported as means \pm standard deviation (SD). P values were calculated by using the unpaired Student's *t* test. The number of replicates in each experiment is indicated in the figure legends.

RESULTS

Isolation and Characterization of CD105⁺ cells from Pulp and Adipose Tissue

Flow cytometric isolation of the CD105⁺ cells from canine adult total pulp cells (Fig. 1D) were performed using antibodies against CD105. CD105⁺ cells isolated from total adipose cells (Fig. 1H) of the same dog and unfractionated total pulp cells were used as controls. The pulp and adipose CD105⁺ cells represented 6% and 5.8% of total cells, respectively (Fig. 1A, E). The CD105⁺ cells from both the pulp and the adipose tissue were stellate with long cell processes (Fig. 1B, C, F, G). The pulp CD105⁻ cells were of varied shapes with short processes. EBM2 supplemented with IGF1, EGF and 10% FBS maintained the phenotype of